Volume 1 | Number 1 | Jan 2013 | Pages 1–100

Dalton Transactions

An international journal of inorganic chemistry
www.rsc.org/dalton

ROYAL SOCIETY OF CHEMISTRY

ROYAL SOCIETY OF CHEMISTRY

www.rsc.org/dalton

Synthesis and Third-Order Nonlinear Optical Properties of Heteroleptic Mo$_3$S$_7$ Clusters

Graphical Abstract

A series of mixed-ligand diimine-halide and diimine-dithiolene clusters based on the Mo$_3$S$_7$ core have been synthesized. Their optical limiting behavior was assessed by Z-scan techniques, and compared to that of a dithiolene Mo$_2$O$_2$S$_2$-based cluster, with the aim of finding correlations between molecular structures and third-order nonlinear optical functions.
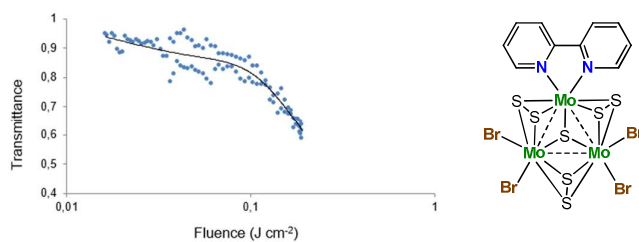
Synthesis and Optical Power Limiting Properties of

Heteroleptic Mo$_3$S$_7$ Clusters

David Recatalá,[a] Rosa Llusar,[*, a] Adam Barlow,[b] Genmiao Wang,[b] Marek Samoc,[c] Mark G. Humphrey[b] and Artem L. Gushchin[a,d,e]

[a] Departament de Química Física i Analítica, Universitat Jaume I, Av. Sos Baynat s/n, 12071 Castelló, Spain

[b] Research School of Chemistry, Australian National University, Canberra, ACT 2601, Australia

[c] Advanced Materials Engineering and Modeling Group, Faculty of Chemistry, Wroclaw University of Technology, 50-370 Wroclaw, Poland

[d] Nikolaev Institute of Inorganic Chemistry, Siberian Branch of the Russian Academy of Sciences, 630090 Novosibirsk, Russia

[e] Novosibirsk State University, 630090 Novosibirsk, Russia

AUTHOR EMAIL ADDRESS: * author for correspondence: rosa.llusar@uji.es

TITLE RUNNING HEAD:

CORRESPONDING AUTHOR FOOTNOTE

[a] Dept. de Química Física i Analítica, Universitat Jaume I, Av. Sos Baynat s/n, 12071 Castelló, Spain: E-mail: rosa.llusar@uji.es; Tel: +34 964728086; Fax: +34 964728066; Homepage: http://www.grupo-rllusar.uji.es

Abstract

Substitution of the halide ligands in $(Bu_4N)_2[Mo_3S_7X_6]$ (X = Cl, Br) by diimine ligands, such as 4,4'-dimethyl-2,2'-bipyridine (dmbpy), 2,2'-bipyridine (bpy) and 1,10-phenanthroline (phen), affords the neutral heteroleptic clusters $Mo_3S_7Cl_4$(dmbpy) (**1**), $Mo_3S_7Br_4$(dmbpy) (**2**), $Mo_3S_7Br_4$(bpy) (**3**), and $Mo_3S_7Br_4$(phen) (**4**). Further substitution of the halide ligands in $Mo_3S_7Br_4$(diimine) clusters by dmit (1,3-dithiole-2-thione-4,5-dithiolate) allows the preparation of the mixed diimine-dithiolene neutral cluster complexes Mo_3S_7(dnbpy)(dmit)$_2$ (**5**, dnbpy = 4,4'-dinonyl-2,2'-bipyridine), Mo_3S_7(dcmbpy)(dmit)$_2$ (**6**, dcmbpy = 4,4'-dimethoxycarbonyl-2,2'-bipyridine), and Mo_3S_7(dcbpy)(dmit)$_2$ (**7**, dcbpy = 2,2'-bipyridine-4,4'-dicarboxylic acid). The optical limiting properties of complexes **1 – 7** have been assessed by the open-aperture Z-scan technique at 570 nm, employing a nanosecond optical parametric oscillator. In order to investigate the effect of increasing the π-system, complexes **1 – 4**, with general formula $Mo_3S_7X_4$(diimine), (X = Cl, Br), were compared to clusters **5 – 7**, containing the dmit ligand. The influence of the metal content on the optical power limiting properties was also investigated by comparing the trinuclear series of complexes prepared herein with the bis(dithiolene) dinuclear cluster $(Et_4N)_2[Mo_2O_2S_2(BPyDTS_2)_2]$, which has been recently prepared by our group. All trinuclear clusters **1 – 7** are efficient optical limiters ($\sigma_{eff} > \sigma_0$) with threshold limiting fluence $F_{15\%}$ decreasing on proceeding from dinuclear to trinuclear clusters and, generally, on extending the π-system.

Introduction

Inorganic materials have been widely used in optics and electronics for many years. With the development of optoelectronics and photonics, the discovery of compounds able to meet the demands of technology has become even more important. In this

2

context, the search for materials with improved third-order nonlinear optical (NLO) properties, which include the phenomena of nonlinear refraction and nonlinear absorption, is of utmost importance. Optimizing such materials will permit further developments in a number of photonic technologies. One such application where the existing materials are still lacking the appropriate performance is optical limiting (power limiting).[1] Optical limiting is a physical phenomenon that involves clamping the optical power transmitted through a material when the incident light intensity increases, which corresponds to the material transmittance decreasing at higher intensities. Power limiting devices based on a variety of materials such as, for example, organic dyes, polymers, inorganic semiconductors, and carbon-based systems like carbon nanotubes or fullerenes have been suggested. A large number of coordination and organometallic molecular complexes that may be useful as NLO materials in photonics have also been reported.[2] Less attention has been devoted to inorganic clusters. This is mainly due to two reasons: on the one hand, their (usually) deep color makes them unsuitable for NLO applications necessitating transparency in the visible region, and on the other hand, their frequent instability in the presence of high intensity radiation prohibits applications involving lasers.[3] However, the past two decades have witnessed significant progress in the field since a series of cubane-like heterobimetallic molybdenum and tungsten cluster sulfides were found to be superior optical limiters to fullerene, C_{60}.[4–6] The presence of bridging sulfide ligands enhances the photochemical stability of metal clusters by reinforcing the metal-metal bonds.

Despite the drawbacks mentioned above, metal clusters present several advantages over other inorganic/organic compounds traditionally used in nonlinear optics. Firstly, their constituent heavy atoms introduce more energy sublevels, and

consequently more allowed transitions, as compared to organic molecules, and secondly, their NLO properties can be easily tuned by changing the constituent elements, oxidation state, structural type and/or outer ligands. Zhang et al. have systematically explored the structure–property correlation within a series of Mo(W)/S(Se)/Ag clusters. Five different skeletal cluster cores have been shown to display significant third-order NLO properties. In addition, two different heavy atom effects on the third-order NLO properties of this system have been identified. Substitution of S by Se causes a stronger NLO performance of the system, while there is a sign alternation from the self-defocusing performance upon replacing Mo by W.[7] Further systematic investigations are needed to establish additional correlations that will ultimately allow us to identify the optimal NLO material.

In the past, our groups have explored the NLO performance of a series of incomplete cuboidal $[M_3(\mu_3\text{-}Q)(\mu_2\text{-}Q)_3X_3(\text{diphosphine})_3]^+$ (M = Mo, W; Q = S, Se; X = Cl, Br) cluster complexes and the closely related $[M_3Cu(\mu_3\text{-}Q)(\mu_2\text{-}Q)_3X_3(\text{diphosphine})_3]^+$ heterometallic cubane-type compounds.[6–18] These trinuclear and tetranuclear complexes are all optical limiters ($\sigma_{eff} > \sigma_0$) with threshold-limiting fluence decreasing on proceeding from tetranuclear to trinuclear, and from W-containing to Mo containing clusters. Power limiting has also been found in $Mo_3(\mu_3\text{-}S)(\mu_2\text{-}S)_3$ cluster sulfides derivatized with maleonitrile dithiolate, oxalate and thiocyanate ligands, although no clear tendencies could be drawn upon ligand substitution.[8] In our search for better NLO materials, we have extended our study to other ligands, namely diimines and dithiolenes. Pyridyl complexes were among the first inorganic molecular NLO materials and they still continue to attract significant interest.[9,10] Furthermore, the

nonlinear optical behavior of dithiolene metal complexes is also of interest since π-extended systems are well-known to enhance the NLO properties of a material.[11,12]

Herein, we report the synthesis of seven novel heteroleptic $Mo_3(\mu_3\text{-}S)(\mu_2\text{-}S_2)_3$ clusters containing either mixed diimine-halide, $Mo_3S_7X_4(\text{diimine})$ (X = Cl, Br), or diimine-dithiolene ligands, $Mo_3S_7(\text{dithiolene})_2(\text{diimine})$. The latter represent the first examples of cluster compounds containing mixed diimine/dithiolene ligands. The optical power limiting properties of all these cluster complexes have been evaluated using the Z-scan technique. The NLO behavior of the previously reported dinuclear cluster $(Et_4N)_2[Mo_2O_2S_2(BPyDTS_2)_2]$ (BPyDTS$_2$ = 2-bis-(2-pyridyl)methylene-1,3-dithiolene)[13] has also been investigated, with the aim of finding correlations between nuclearity and third-order optical functions.

Results and discussion

Synthesis and structure of neutral $Mo_3S_7X_4(\text{diimine})$ complexes. Homoleptic $Mo_3(\mu_3\text{-}S)(\mu_2\text{-}S_2)_3$ clusters functionalized with a large variety of ligands, such as thiocyanate, dithiocarbamate, catecholate, dithiolene, etc., are readily accessible by ligand substitution reactions starting from the $[Mo_3S_7Br_6]^{2-}$ complex.[8,14–16] In the case of the dithiolene Mo_3S_7 derivatives, upon oxidation these cluster compounds have been used to prepare single molecule magnetic molecular conductors.[14] Surprisingly, reaction of this precursor with 1,10-phenanthroline or bipyridine derivatives only causes replacement of two bromides on the same metal atom, and affords heteroleptic $Mo_3S_7Br_4(\text{diimine})$ neutral compounds. The 1,10-phenanthroline derivatives are luminescent materials with potential applications as sensors while the bipyridine clusters adsorbed on titanium oxide nanoparticles are precatalysts in photocatalytic

5

hydrogen evolution processes.[17] In this work, we have extended this ligand substitution synthetic route, represented in equation 1, to other diimine ligands, namely 4,4'-dimethyl-2,2'-bipyridine (hereinafter, dmbpy), 2,2'-bipyridine (bpy) or 1,10-phenanthroline (phen).

$$[Mo_3S_7X_6]^{2-} + \text{diimine} \rightarrow Mo_3S_7X_4(\text{diimine}), \text{ with X = Cl or Br} \quad (1)$$
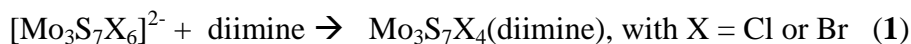
Scheme 1 shows the molecular structure of the four isolated $Mo_3S_7X_4$(diimine) clusters: $Mo_3S_7Cl_4$(dmbpy) (**1**), $Mo_3S_7Br_4$(dmbpy) (**2**), $Mo_3S_7Br_4$(bpy) (**3**), and $Mo_3S_7Br_4$(phen) (**4**).

X = Cl ; **1**
X = Br ; **2**

X = Br ; **3**

X = Br ; **4**
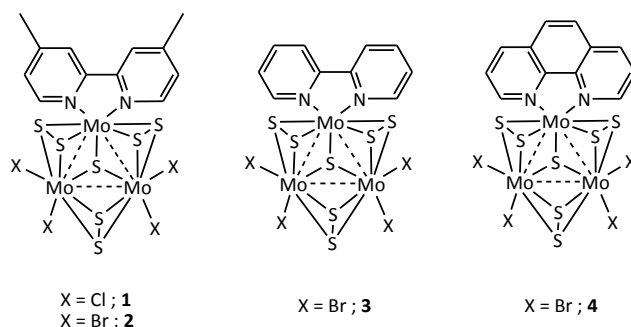
Scheme 1. Molecular structure of complexes **1 – 4**.

In order to facilitate the characterization of the highly insoluble neutral $Mo_3S_7X_4$(diimine) complexes, we took advantage of the electrophilic character of the axial μ-S_2^{2-} ligands and their tendency to form anionic $\{Mo_3S_7X_4(\text{diimine}).X\}^-$ aggregates.[18–25] Clusters **1 – 4** could be redissolved in dichloromethane and crystallized in the presence of an excess of Bu_4NCl (complex **1**) or Bu_4NBr (complexes **2 – 4**) by slow diffusion methods (see Experimental Section). Single crystals of compounds $(Bu_4N)[\textbf{1}\cdot\textbf{Cl}]$, $(Bu_4N)[\textbf{2}\cdot\textbf{Br}]$, $(Bu_4N)[\textbf{3}\cdot\textbf{Br}]$ and $(Bu_4N)[\textbf{4}\cdot\textbf{Br}]$ were obtained by slowly diffusing toluene into sample solutions in dichloromethane. The solid-state structures of the cluster complexes were determined by X-ray diffraction.

Figures 1 shows the ORTEP representation of structure (Bu$_4$N)[**1**·Cl], as representative example of all four structures, with the atom numbering scheme. All these heteroleptic molybdenum clusters crystallize as tetra-*n*-butylammonium salts of anionic aggregates in which neutral cluster molecules of [Mo$_3$(μ_3-S)(μ_2-S$_2$)$_3$X$_4$L] (X = Cl or Br; L = bpy, phen or dmbpy) participate in non-valence interactions between the sulfur axial atoms (S(3), S(5) and S(7) in Figure 1) and a chloride/bromide anion. The two nitrogen atoms of the diimine ligand are coordinated to one of the Mo atoms in a chelating mode (average Mo-N distance of 2.216(7) Å), and the plane defined by the ligand is oriented almost perpendicularly to the trimetallic plane. The S$_{ax}$…Cl contacts (average length 2.93(4) Å) or S$_{ax}$…Br interactions (average length 3.04(9) Å) can be explained by the electrophilic character of the sulfur atoms that lie in the axial plane. These kinds of interactions are also observed in related cluster compounds.[18–25] Intracluster metal-metal and metal-sulfur bond distances are consistent with those for an oxidation state of +4 for the metal, and the presence of single metal-metal bonds (see Table 1).[18–25] In addition to the crystal structure determinations, the identities of complexes (Bu$_4$N)[**1 – 4**] were confirmed by mass spectrometry.
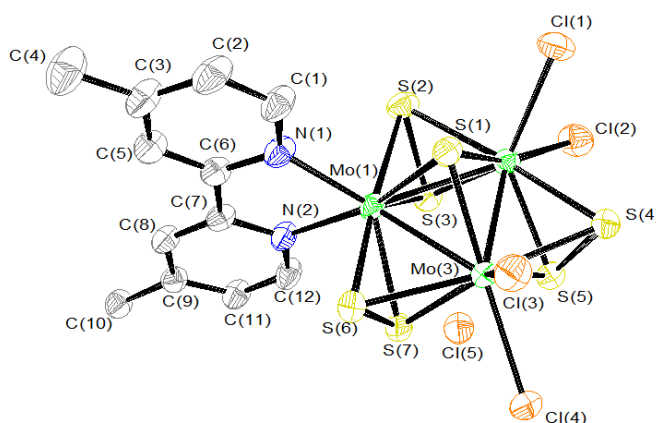

Figure 1. ORTEP representation (50 % probability ellipsoids) of the anionic trinuclear cluster [**1**·Cl]⁻ with the atom numbering scheme.

7

Synthesis of Mo_3S_7(diimine)(dithiolene)$_2$ complexes. With the aim of extending the chemistry of the $Mo_3S_7X_4$(diimine) (X = Cl, Br) complexes, the previously reported clusters $Mo_3S_7Br_4$(dnbpy) (dnbpy = 4,4'-dinonyl-2,2'-bipyridine) and $Mo_3S_7Br_4$(dcmbpy) (dcmbpy = 4,4′-dimethoxycarbonyl-2,2′-bipyridine)[17] were reacted with $(Bu_4N)_2[Zn(dmit)_2]$ (dmit = 1,3-dithiole-2-thione-4,5-dithiolate), the zinc complex of the dmit ligand.[26,27] In this way, the neutral complexes Mo_3S_7(dnbpy)(dmit)$_2$ (**5**) and Mo_3S_7(dcmbpy)(dmit)$_2$ (**6**) were obtained. Complex Mo_3S_7(dcbpy)(dmit)$_2$ (**7**, dcbpy = 2,2'-bipyridine-4,4'-dicarboxylic acid) was prepared *in situ* without prior isolation of the $Mo_3S_7Br_4$(dcbpy) complex due to the extremely low solubility of this intermediate in organic solvents, such as dimethylformamide or dimethyl sulfoxide. The approach used for the synthesis of complexes **5 – 7** is summarized in Scheme 2.

R = C_9H_{19}, **5**
R = $COOCH_3$, **6**
R = COOH, **7**
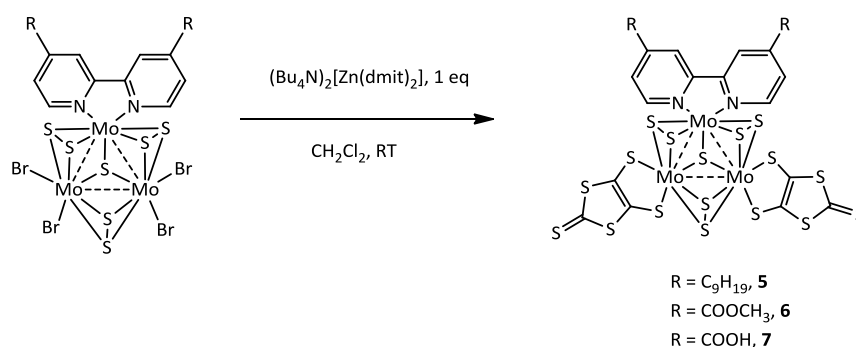
Scheme 2. Synthetic pathway for complexes **5 – 7**.

Zinc complexes containing dithiolene ligands have been widely used by our group as masked forms of dithiolates which allow the synthesis of tris(dithiolene) trinuclear molybdenum clusters by transmetalation.[14–16] Apart from helping in the stabilization of the dithiolate ligand, their use is very convenient since Mo_3S_7 cluster

units are not stable under the basic conditions that are usually required for the coordination of dithiolene ligands.

Despite being soluble in the reaction mixture, after isolation all resulting neutral products (with the exception of complex **5**) were insoluble in common organic solvents. It is well-known that in $[Mo_3(\mu_3\text{-}S)(\mu\text{-}S_2)_3]^{4+}$ units the sulfur atoms that lie in the axial plane are slightly electrophilic, and consequently can interact with nucleophilic anions, such as the chloride/bromide ligands replaced by the diimine or dithiolene ligands during the substitution reaction.[18–25] Consequently, tetra-*n*-butylammonium salts of $[Mo_3S_7X_4(\text{diimine})\cdot X]^-$ (X = Cl, Br) or $[Mo_3S_7(\text{diimine})(\text{dithiolene})_2\cdot X]^-$ complexes may be present in solution, which explains the high solubility of the complexes in the reaction mixture. During the purification process such electrostatic interactions were presumably broken, leading to neutral $Mo_3S_7(\text{diimine})(\text{dithiolene})_2$ complexes, exhibiting poor solubility in common organic solvents.

The low solubility of complexes **5 – 7** in common organic solvents limited the number of techniques employed for their characterization. Unfortunately, thus far all attempts to grow single crystals of these compounds suitable for X-ray structural analysis have been unsuccessful. Additionally, the identities of complexes **5 – 7** could not be confirmed from the ESI-MS spectra since it was not possible to ionize them. Alternative techniques (elemental analysis, infrared and UV/Vis spectroscopies) have been used to prove the purity of these products.

In all complexes, there is a good correlation between the calculated and experimental compositions for carbon, hydrogen, nitrogen and sulfur. The characteristic bands of the Mo_3S_7 units, as well as those of their outer diimine and dithiolene ligands were observed in the IR spectra of complexes **5 – 7**. These bands were identified on the

9

basis of the stretching frequencies reported for similar cluster complexes.[28–31] In all cases, a weak band corresponding to the $S_{eq} - S_{ax}$ stretching vibration was observed at *ca.* 516 cm^{-1}. The vibrations of the Mo - μ_3S bonds were observed in the form of multiple bands in the 416 – 420 cm^{-1} range. The multiple signals corresponding to the C=C stretching vibrations of the bipyridine rings appear in the range of 1417 – 1613 cm^{-1}. The bands assigned to the C=S vibrations of the dmit ligand were found in all cases at 1053 cm^{-1}. In addition, further bands were observed due to the vibration of the atoms of the groups appended to the functionalized bipyridine ligands. For instance, in complex **5**, the Csp^3-H vibration bands of the long alkyl chains in the ligand were found in the range of 2849 – 2920 cm^{-1}. In complex **6** the vibrations of the C=O and C-O groups were observed as two single bands at 1732 cm^{-1} and 1267 cm^{-1}, respectively. Finally, in complex **7**, containing the analogous dcbpy ligand, apart from the C=O and C-S bands discussed for complex **6**, the vibrations of the terminal O-H groups were found as a broad band centered at 3446 cm^{-1}.

Optical Limiting Properties. The linear optical and optical power limiting properties of clusters **1** – **7** were examined. Linear optical spectra are displayed in Figures 2 and 3, respectively. Important spectral data are listed in Table 2. When we were able to examine the clusters across a range of solvents of different polarities (dichloromethane, tetrahydrofuran, dimethylformamide), they exhibited significant solvatochromism. This was not explored further due to variable solubility in the less polar solvents, and consequently the studies summarized below were undertaken in dimethylformamide.
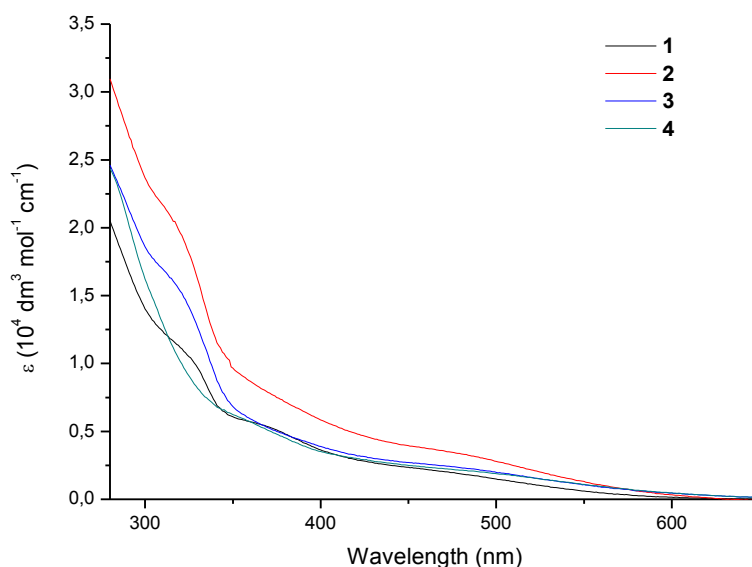
Figure 2. Linear optical spectra for complexes **1** – **4** in dimethylformamide solution.

The UV-visible spectra of complexes **1** – **7** reveal intense bands at highest energy (λ_1, 304-342 nm), less intense bands at lower energy (λ_2, 335-427 nm), and weak bands at lowest energy (λ_3, 446-538 nm). The cluster $(Et_4N)_2[Mo_2O_2S_2(BPyDTS_2)_2]$ is structurally distinct,[13] possessing an $Mo_2(\mu_2\text{-}S)_2(O)_2$ core, in contrast to the other heteroleptic complexes which possess $Mo_3(\mu_3\text{-}S)(\mu_2\text{-}S_2)_3$ cores; its absorption maxima are at lowest energy across the series of complexes presented in this work. For the latter, the lowest energy (λ_3) bands follow the wavelength order: complex **7** > complex **5** > complex **6** = complex **4** > complex **3** > complex **2** > complex **1**, with the dmit (1,3-dithia-2-thione-4,5-dithiolate) ligated clusters **5** – **7** exhibiting the lowest energy maxima, and the chloro-ligated cluster **1** exhibiting the highest energy maximum.

11
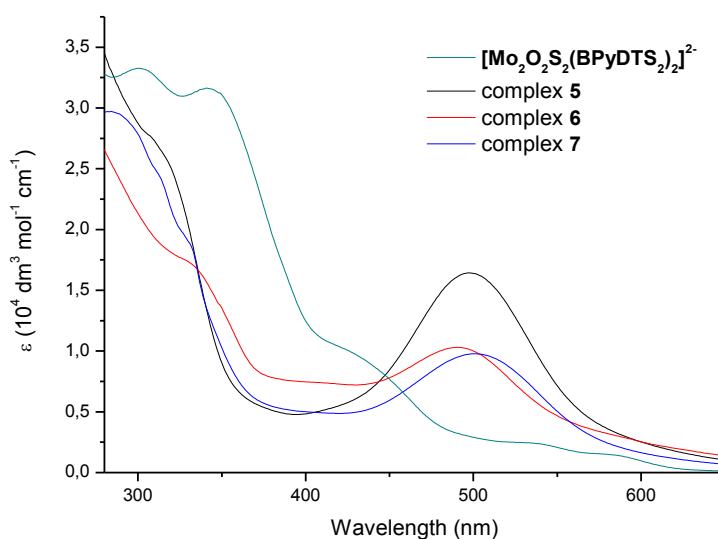
Figure 3. Linear optical spectra for complexes $(Et_4N)_2[Mo_2O_2S_2(BPyDTS_2)_2]$[13] and **5 – 7** in dimethylformamide.

The UV-visible spectra of the eight clusters contain broad low-intensity absorptions through areas of the visible region of the spectrum, suggestive of potential as broad-band optical limiters. Relevant data for optical limiting merit from Z-scan measurements (see Experimental) are collected in Table 2. All clusters absorb weakly at the specific wavelengths chosen to assess their optical limiting performance.

Insert Table 2

As we have discussed previously, closed-aperture Z-scan is usually used to derive the nonlinear refractive index n_2 by examining self-focusing or self-defocusing phenomena, while open-aperture Z-scan can afford the nonlinear absorption properties by monitoring the total transmission through a sample.[32] Both were employed in the present studies. The closed-aperture scans show characteristic self-defocusing traces. The negative refractive nonlinearity may possess contributions from a variety of

Dalton Transactions Accepted Manuscript

12

different mechanisms, including thermal effects. Therefore, no further comment is made here.

Transmission vs. fluence plots were generated, where the fluence is the energy of the laser pulse per unit area. Examples of each class of complex are shown in Figure 4. For comparative purposes, a threshold limiting fluence $F_{15\%}$ (defined as the incident fluence needed to reduce the transmittance through a sample by 15%) has been used to assess the relative optical limiting merit of these clusters. The results are tabulated in Table 2.

13

(a)

(b)

(c)
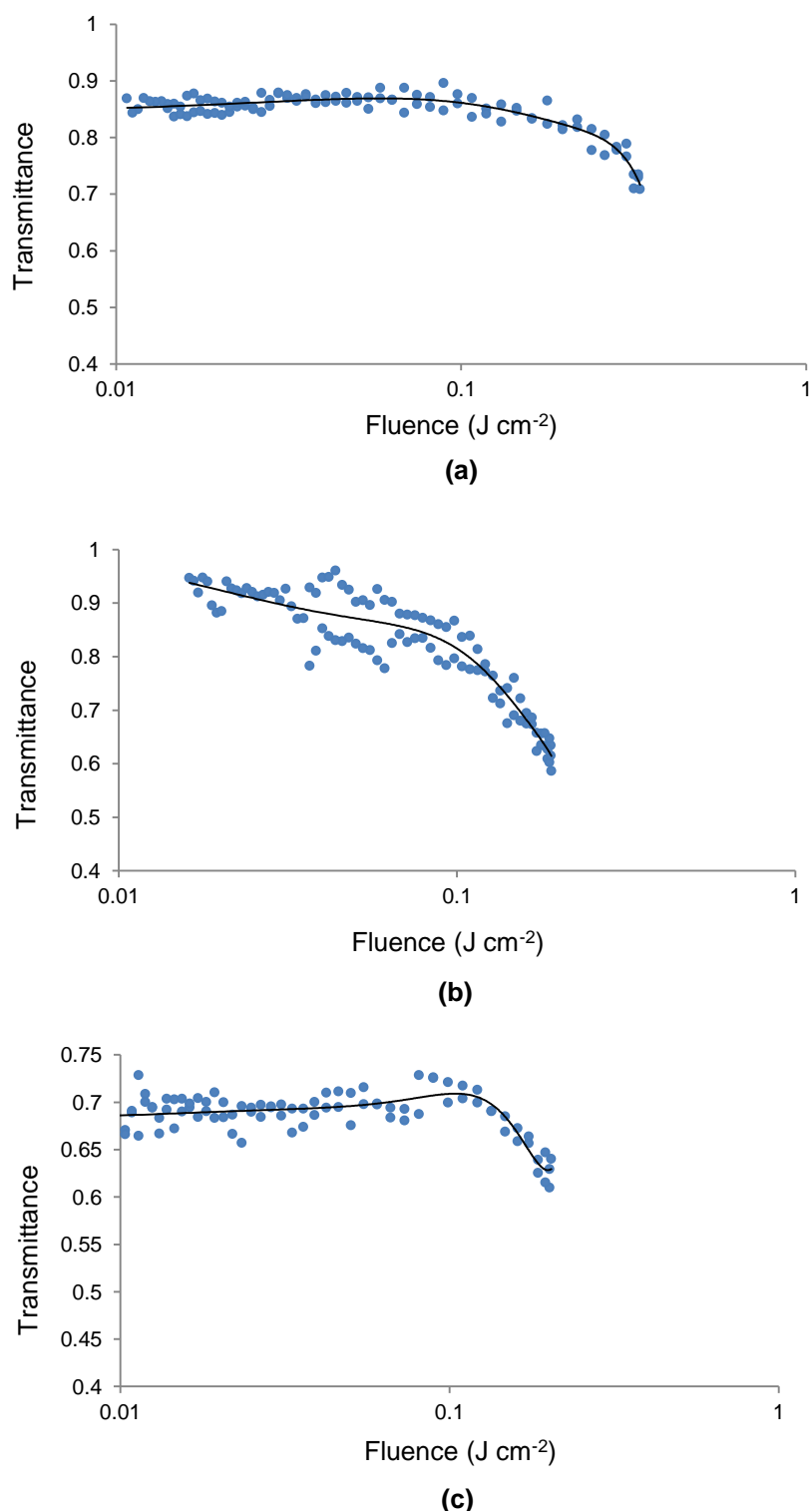
Figure 4. Optical limiting behavior of (a) (Et$_4$N)$_2$[Mo$_2$O$_2$S$_2$(BPyDTS$_2$)$_2$][13], (b) complex

3, and (c) complex **5**.

14

The threshold limiting fluences at 570 nm follow the trend: complex **3** $\approx$ complex **2** < complex **5** $\approx$ complex **7** = complex **4** < complex **6** < complex **1** < $[Mo_2O_2S_2(BPyDTS_2)_2]^{2-}$. The optical limiting merit therefore increases on increasing the metal content (proceeding from dinuclear $[Mo_2O_2S_2(BPyDTS_2)_2]^{2-}$ to the trinuclear clusters). Assuming a three-state reverse saturable absorption model and employing literature expressions, effective cross-sections of the dominant excited states can be calculated.[33] The energy transmittance of the cell with a Gaussian beam is given by:

$$T = (1 - R)^2 \frac{\exp(-a_0 L)}{q} \ln(1 + q)$$

where

$$q = (1 - R)[1 - \exp(-a_0 L)] d_{\text{eff}} F_0 / 2F_s$$

and R is the reflection coefficient, α_0 is the low power absorption coefficient, F_0 is the fluence and F_s is the saturation fluence defined as:

$$F_s = \frac{\hbar w}{S_0}$$

and

$$d_{\text{eff}} = \frac{S_{\text{eff}} - S_0}{S_0}$$

where σ_{eff} is the effective excited-state cross-section and σ_0 is the ground-state cross-section. Note that these expressions are derived assuming that the lifetime of the state active in the reverse saturable absorption process is longer than the laser pulse duration. Note also that the effective excited-state cross section should only be treated as a measure of the power limiting ability of the substance under specific experimental

15

conditions; it may contain contributions from several different excited states with different properties (e.g. from states of different spin). The values of the excited-state cross-sections σ_{eff} for the clusters are given in Table 1. With the exception of the dinuclear cluster $[Mo_2O_2S_2(BPyDTS_2)_2]^{2-}$, the σ_{eff} values are larger than those of the corresponding ground-state cross-sections σ_0. In other words, all trinuclear clusters in the present study are optical limiters.

Cluster **6** was also examined at 500, 532, and 640 nm, in addition to the aforementioned measurement at 570 nm. For **6**, σ_{eff} and σ_{eff}/σ_0 data vary with the wavelength of study. At the shorter wavelengths, the ground-state cross-sections are larger than the excited-state cross-sections, and the cluster no longer functions as an optical limiter. These data are consistent with **6** (and by implication the other clusters in the present study) functioning as an optical limiter via an RSA mechanism at longer wavelengths (including the benchmark wavelength of 570 nm).

The values of σ_{eff} derived in the present experiments can in principle be compared to those presented by us before,[8,32,34] but comparisons between values obtained in these different data collection runs should be cautious, since the effective cross section values are likely to depend to a certain degree on the details of a power limiting experiment such as the pulse duration, the geometric parameters of the laser beam, etc. Comparison between data collected in different laboratories should be even more circumspect. We have sought to benchmark the present data against well-studied materials. Under our conditions, Rhodamine B in acidified DMF proved to be photosensitive (bleaching was observed). C_{60} as a suspension in DMF (σ_0 1.8 x 10^{-18} cm^{-2}, σ_{eff} 33.0 x 10^{-18} cm^2, σ_{eff}/σ_0 18.1) proved more efficient than the clusters, but further comment is not warranted as the suspension of C_{60} in our study is likely to be

16

functioning as an optical limiter largely by scattering, rather than attenuation by excited-state absorption.

The present σ_{eff} data (complex **5** > complex **6** > complex **7** > complex **4** ≈ complex **2** ≈ complex **3** > complex **1**) are suggestive that extending the π-delocalization (by introducing dmit ligands) and lowering the energy of the π-system of the bipyridine ligands in the series (by appending electron-withdrawing carboxylic acid or methyl ester groups), leads to an improvement in σ_{eff}. While minimizing speculative interpretation, this is consistent with the relevant excited states having significant ligand character, and with tuning of the energy levels being a key determinant of optical limiting merit. Further comment on the optical power-limiting mechanism requires time-resolved experiments.

Experimental Section

General Procedures. Elemental analysis was performed on an EA 3000 CHN analyser. ^{1}H-NMR spectra were recorded on a Varian Mercury Vx 300 MHz instrument, using deuterated solvents, and were referenced to internal tetramethylsilane. IR spectra were recorded in the 400–4000 cm^{-1} range on a Jasco 6200 FT/IR spectrometer using KBr pellets. Characteristic IR bands were assigned on the basis of those of previously reported complexes. Electronic spectra in the different solvents were recorded on a Hewlett-Packard UV/Vis 8453 spectrophotometer. Electrospray ionization mass spectra were recorded on a triple quadrupole mass spectrometer (Micromass Quattro LC). The chemical composition of each peak in the scan mode was assigned by comparing the

isotope experimental pattern with that calculated using the MassLynx 4.1 program. Unless otherwise stated, all synthetic reactions were carried out under nitrogen-gas atmosphere using standard Schlenk techniques. High-purity solvents for synthesis were used. Dichloromethane was further purified by using an MBRAUN SPS-800 system. N,N-dimethylformamide (DMF) was degassed *in vacuo*.

Optical Limiting Studies. Optical measurements were performed on dimethylformamide solutions of samples placed in 1 mm glass cells. Linear optical spectra were obtained on a Varian Cary 5 spectrophotometer over the spectral range 270-800 nm at the Research School of Chemistry (RSC), Australian National University (ANU). The light source used for the determination of power limiting properties was an Opolette (HE) 355 II (Opotek), located at RSC, ANU. This is a single-housing tuneable ns laser system in which the third harmonic from a Nd:YAG laser (355 nm pump wavelength, 20 Hz repetition rate, 5 ns pulse length) pumps an OPO (tuning range 410-2200 nm, peak OPO energy 10 mJ, spectral linewidth 4-7 cm^{-1}). The optical power limiting experiments were performed on solutions of concentrations 0.07-0.35% w/w. The properties were assessed by the open-aperture Z-scan technique at 570 nm at which the samples had low, but non-zero, linear absorption (corresponding to ε values of 307-4411 M^{-1} cm^{-1} at the measurement wavelength). Additional studies of cluster **6** were undertaken at 500, 532, and 640 nm. The data from the power limiting curves obtained by the open-aperture Z-scan technique were then converted into transmittance-fluence plots assuming a Gaussian character of the beam, the w_0 parameter of the beam being determined from closed-aperture Z-scan results. The clusters were tested and found to be photochemically stable at light intensities up to 65 MW cm^{-2}, as judged by the symmetrical nature of the Z-scan curve.

18

Starting Materials. Commercially available starting materials (4,4'-dimethyl-2,2'-bipyridine, 2,2'-bipyridine and 1,10-phenanthroline) were obtained either from Sigma-Aldrich or Acros, and used as received without further purification. The preparation of the ligand 2,2'-bipyridine-4,4'-dicarboxylic acid is described elsewhere.[35] The complex $(TBA)_2[Zn(dmit)_2]$ was synthesized by following the approach described by Steimecke.[26,27] The thioclusters $(Bu_4N)_2[Mo_3S_7Br_6]$ and $(Bu_4N)_2[Mo_3S_7Cl_6]$ were prepared from $(NH_4)_2[Mo_3S_{13}] \cdot nH_2O$[36] as described previously[37], but using Bu_4NBr and Bu_4NCl, respectively, to precipitate the final compound. The complexes $Mo_3S_7Br_4(dnbpy)$, $(Bu_4N)[Mo_3S_7Br_5(dcmbpy)]$[17] and $(Et_4N)_2[Mo_2O_2S_2(BPyDTS_2)_2]$[13] were prepared by our group in the past.

$Mo_3S_7Cl_4$(dmbpy) (1). The cluster $(Bu_4N)_2[Mo_3S_7Cl_6]$ (100 mg, 0.083 mmol) and 4 equivalents of commercial 4,4'-dimethyl-2,2'-bipyridine (62 mg, 0.33 mmol) were mixed with CH_2Cl_2 (20 mL) and heated to reflux for 1 day. The reddish-orange solution was taken to dryness by rotary evaporation. The orange residue was washed with methanol, a few mL of acetonitrile and dichloromethane, and finally diethyl ether. An orange powder was obtained. Yield: 67 mg (96 %). ESI-MS (CH_2Cl_2/CH_3CN, 20 V, −): m/z = 874.3 [MCl]⁻. Elemental analysis (%) calcd. for $C_{12}H_{12}Cl_4Mo_3N_2S_7$: C, 17.19; H, 1.44; N, 3.34; found C, 17.5; H, 1.76; N, 3.45. UV/Vis (DMSO): λ_{max} (ε) = 381 (1654), 447 (1056) nm ($M^{-1}cm^{-1}$).

$Mo_3S_7Br_4$(dmbpy) (2). The starting material $(Bu_4N)_2[Mo_3S_7Br_6]$ (100 mg, 0.068 mmol) and an excess of 4,4'-dimethyl-2,2'-bipyridine (50 mg, 0.27 mmol) were mixed with CH_2Cl_2 (30 mL) and stirred overnight at room temperature. The reddish-orange solution was filtered and taken to dryness by rotary evaporation. The solid residue was washed with methanol, acetonitrile and diethyl ether to afford an orange powder. Yield: 57 mg

19

(82 %). ^{1}H-NMR (d_6-DMSO, 300 MHz): 2.59 (s, 6H), 7.73 (m, 2H), 8.78 (m, 2H), 9.19 (d, 1H), 9.57 ppm (m, 1H). ESI-MS (CH_2Cl_2/CH_3CN, 20 V, −): m/z = 1096.0 [MBr]$^-$, 1052.3 [MCl]$^-$, 1006.3 [M - Br + 2Cl]. Elemental analysis (%) calcd. for $C_{12}H_{12}Br_4Mo_3N_2S_7$: C, 14.18; H, 1.19; N, 2.76; found C, 14.3; H, 1.4; N, 2.4. UV/Vis (DMSO): λ_{max} (ϵ) = 450 (2389) nm ($M^{-1}cm^{-1}$).

$Mo_3S_7Br_4$(bpy) (3). The complex $(Bu_4N)_2[Mo_3S_7Br_6]$ (100 mg, 0.068 mmol) and an excess of 2,2'-bipyridine (53 mg, 0.34 mmol) were stirred overnight at room temperature. The red mixture was filtered, and the filtrate was taken to dryness by rotary evaporation. The sticky solid residue was washed with methanol, acetonitrile, dichloromethane and diethyl ether. An orange solid was obtained. Yield: 45 mg (67 %). ^{1}H-NMR (d_6-DMSO, 300 MHz): 7.91 (m, 2H), 8.48 (q, 2H), 8.91 (m, 2H), 9.36 (d, 1H), 9.81 ppm (d, 1H). ESI-MS (CH_2Cl_2/CH_3CN, 20 V, −): m/z = 1068.0 [MBr]$^-$, 1024.0 [MCl]$^-$, 979.1 [M − Br + 2Cl]$^-$. Elemental analysis (%) calcd. for $C_{10}H_8Br_4Mo_3N_2S_7$: C, 12.16; H, 0.82; N, 2.84; found C, 12.40; H, 1.10; N, 2.85. UV/Vis (DMSO): λ_{max} (ϵ) = 458 (2258) nm ($M^{-1}cm^{-1}$).

$Mo_3S_7Br_4$(phen) (4). The cluster species $(Bu_4N)_2[Mo_3S_7Br_6]$ (100 mg, 0.068 mmol) and 5 equivalents of commercially available 1,10-phenanthroline (62 mg, 0.34 mmol) were allowed to stir overnight at room temperature. After removing the orange precipitate by filtration, the red filtrate was taken to dryness. The reddish-orange solid was thoroughly washed with methanol, acetonitrile, dichloromethane and diethyl ether. Yield: 55 mg (69 %). ^{1}H-NMR (d_6-DMSO, 300 MHz): 8.27 (m, 2H), 8.41 (s, 2H), 9.13 (m, 2H), 9.65-9.80 (m, 1H), 10.12 ppm (m, 1H). ESI-MS (CH_2Cl_2/CH_3CN, 20 V, −): m/z = 1092.0 [MBr]$^-$, 1048.0 [MCl]$^-$. Elemental analysis (%) calcd. for

$C_{12}H_8Br_4Mo_3N_2S_7$: C, 14.24; H, 0.80; N, 2.77; found C, 14.55; H, 1.30; N, 2.65. UV/Vis (DMSO): λ_{max} (ε) = 453 (3149) nm ($M^{-1}cm^{-1}$).

Mo_3S_7(dnbpy)(dmit)$_2$ (5). To a solution of $Mo_3S_7Br_4$(dnbpy) (300 mg, 0.24 mmol) in CH_2Cl_2 (75 mL), 1.1 equivalents of $(Bu_4N)_2[Zn(dmit)_2]$ (252 mg, 0.27 mmol) were added. The solution was stirred for 6 h at room temperature. The dark red mixture was filtered, and the filtrate was taken to dryness by rotary evaporation. The sticky dark residue was thoroughly washed with methanol, water, acetonitrile, and diethyl ether. A dark powder was obtained. The reaction is almost quantitative. Yield: 315 mg (99 %). Elemental analysis (%) calcd. for $C_{34}H_{44}Mo_3N_2S_{17}$: C, 31.09; H, 3.38; N, 2.13; S, 41.50; found C, 31.3; H, 3.7; N, 2.1; S, 41.2. IR (KBr, cm^{-1}): 2920 (s, Csp^3-H); 2849 (s, Csp^3-H); 1613 (m, C=C); 1542 (w, C=C); 1457 (m, C=C); 1417 (m, C=C); 1053 (s, C=S); 1023 (s, C-S); 516 (w, S_{eq}-S_{ax}); 420 (w, Mo-μS_3). UV/Vis (DMSO): λ_{max} (ε) = 326 sh (17 550), 492 (11 665) nm ($M^{-1}cm^{-1}$).

Mo_3S_7(dcmbpy)(dmit)$_2$ (6). To a solution of $(Bu_4N)[Mo_3S_7Br_5$(dcmbpy)] (360 mg, 0.25 mmol) in CH_2Cl_2 (60 mL), solid $(Bu_4N)_2[Zn(dmit)_2]$ (240 mg, 0.25 mmol) was added in one portion. The dark purple mixture was stirred for 6.5 h at room temperature. After filtration, the solution was taken to dryness by rotary evaporation. The sticky dark residue was thoroughly washed with methanol, water, hot acetonitrile (until colorless filtrate), and diethyl ether. A dark powder, insoluble in common organic solvents, was obtained. Yield: 240 mg (82 %). Elemental analysis (%) calcd. for $C_{20}H_{12}Mo_3N_2O_4S_{17}$: C, 20.40; H, 1.03; N, 2.38; found C, 20.4; H, 1.3; N, 2.4. IR (KBr, cm^{-1}): 1732 (s, C=O); 1617 (m, C=C); 1542 (w, C=C); 1437 (m, C=C); 1267 (m, C-O); 1053 (s, C=S); 1029 (s, C-O); 517 (w, S_{eq}-S_{ax}); 420 (w, Mo-μS_3). UV/Vis (DMSO): λ_{max} (ε) = 326 sh (6730), 490 (4513) nm ($M^{-1}cm^{-1}$).

21

Mo$_3$S$_7$(dcbpy)(dmit)$_2$ (7). The synthesis of complex **7** was carried out in two steps. The cluster complex (Bu$_4$N)$_2$[Mo$_3$S$_7$Br$_6$] (500 mg, 0.34 mmol) and 5.5 equivalents of 2,2'-bipyridine-4,4'-dicarboxylic acid (460 mg, 1.88 mmol) were mixed with degassed DMF (100 mL). The mixture was heated to 125-130 ºC for 20 h. The red solution, presumably containing the species (Bu$_4$N)[Mo$_3$S$_7$Br$_5$(dcbpy)], was allowed to cool to room temperature. The excess of the ligand precipitated as a white crystalline solid, which was not removed. To this suspension, 1.1 equivalents of solid (Bu$_4$N)$_2$[Zn(dmit)$_2$] (353 mg, 0.37 mmol) were added. The deep purple mixture was stirred overnight at room temperature. The white solid was removed by filtration, and the filtrate was concentrated by rotary evaporation. The solution was cooled to -30 ºC to allow the complete precipitation of the excess of the ligand. After filtration, the solution was taken to dryness by rotary evaporation. Then the dark residue was thoroughly washed with methanol, water, hot acetonitrile and diethyl ether to afford a dark powder, insoluble in common organic solvents. Yield: 290 mg (74 %). Elemental analysis (%) calcd. for C$_{18}$H$_8$Mo$_3$N$_2$O$_4$S$_{17}$: C, 18.81; H, 0.70; N, 2.44; found C, 18.5; H, 1.0; N, 2.5. IR (KBr, cm^{-1}): 3446 (br, OH); 1716 (m, C=O); 1542 (m, C=C); 1458 (m, C=C); 1053 (s, C=S); 516 (w, S$_{eq}$-S$_{ax}$); 416 (m, Mo-μS$_3$). UV/Vis (DMSO): λ_{max} (ε) = 336 sh (12 181), 484 (5475) nm (M^{-1}cm^{-1}).

Structural Determination. Diffraction data for compounds (Bu$_4$N)[**1**·Cl]·3CH$_2$Cl$_2$, (Bu$_4$N)[**2**·Br]·(1/6)CH$_3$C$_6$H$_5$·(1/2)CH$_2$Cl$_2$,   (Bu$_4$N)[**3**·Br]·CH$_3$C$_6$H$_5$·CH$_2$Cl$_2$ and (Bu$_4$N)[**4**·Br] were collected at 200 K on an Agilent Supernova diffractometer equipped with an Atlas CCD detector.[38] For structures (Bu$_4$N)[**1**·Cl], (Bu$_4$N)[**2**·Br] and (Bu$_4$N)[**3**·Br] Mo-Kα radiation (λ = 0.71073 Å) was used, whereas for structure (Bu$_4$N)[**4**·Br], Cu-Kα radiation (λ = 1.54180 Å) was employed. No instrument or crystal

instabilities were observed during data collection. Absorption corrections based on the multi-scan method were applied.[39] All structures were solved by charge-flipping methods using Superflip[40] and refined by the least squares method using SHELXL-2013.[41] Olex2 1.2 software package was used for both the solution and the refinement of the structures.[42] The crystallographic data collection and structure refinement parameters are given in Table 3.

<div align="center">Insert Table 3</div>

In all structures, the non-hydrogen atoms were refined anisotropically. Despite some exceptions, the hydrogen atoms bonded to carbon were included at their idealized positions and refined as riders with isotropic displacement parameters assigned as 1.2 times the U_{eq} value of the corresponding bonding partner. The structure of $(Bu_4N)[\textbf{1}\cdot Cl]$ was refined according to the monoclinic space group $P2_1/n$. Dichloromethane was found cocrystallized with the cluster complex. Compound $(Bu_4N)[\textbf{2}\cdot Br]$ was refined according to the triclinic space group $P\text{-}1$. Dichloromethane and toluene were found cocrystallized with the cluster complex. In the dichloromethane molecule centered at $C(40)$, one chlorine atom was found disordered between two positions and therefore the hydrogen atoms were not included. The sum of the occupation factors of the chlorine atoms was constrained to 1 and their U_{ij} parameters were equated. Structure $(Bu_4N)[\textbf{3}\cdot Br]$ was refined according to the monoclinic space group $P2_1$. Dichloromethane and toluene were also found cocrystallized. In the tetrabutylammonium anion centered at $N(200)$, one terminal carbon was found to be disordered over two positions. Consequently, their occupation factors were expressed in terms of a "free variable" so that their sum was constrained to 1 and their U_{ij} parameters were equated using the EADP constraint. Owing to disorder, we considered as justified the omission of the hydrogen atoms in this

molecule. Finally, the cluster complex (Bu$_4$N)[**4**·Br] was refined according to the triclinic space group P-1. In the tetrabutylammonium cation, three terminal carbons (C104, C108 and C112) were refined with a partial occupancy (0.5, 0.5 and 0.75, respectively). Additionally, the bond distances between three pairs of terminal atoms (C103-C104, C107-C108 and C111-C112) were constrained to a fixed value. The structural figures were drawn by using ORTEP3 v2.02.[43]

Conclusions. In conclusion, novel heteroleptic trinuclear molybdenum cluster complexes containing either mixed diimine-halides or diimine-dithiolene ligands have been prepared and characterized. Their optical power limiting properties have also been investigated and compared to those exhibited by a bis(dithiolene) dinuclear molybdenum cluster prepared formerly by our group, namely (Et$_4$N)$_2$[Mo$_2$O$_2$S$_2$(BPyDTS$_2$)$_2$].[13] The optical limiting merit increases on increasing metal content, and in most cases it increases when the π-system is extended by coordination of dmit, an electron-rich ligand. All trinuclear clusters presented herein are optical limiters with σ$_{eff}$ values larger than those of the corresponding ground-state cross-sections σ$_0$.

Supporting Information. CCDC reference numbers: 1034704 ((Bu$_4$N)[**1**·Cl]), 1034701 ((Bu$_4$N)[**2**·Br]), 1034702 ((Bu$_4$N)[**3**·Br]) and 1034703 ((Bu$_4$N)[**4**·Br]). These data can be obtained free of charge from The Cambridge Crystallographic Data Centre via www.ccdc.cam.ac.uk/data_request/cif

References

1   R. W. Boyd, *Nonlinear Optics*, Elsevier, 2008.

2   M. G. Humphrey, T. Schwich, P. J. West, M. P. Cifuentes and M. Samoc, in *Comprehensive Inorganic Chemistry II*, Elsevier, 2013, pp. 781–835.

3   S. Shi, in *Optoelectronic Properties of Inorganic Compounds*, eds. D. M. Roundhill and J. P. Fackler, Springer US, 1999, p. 412.

4   C. Zhang, Y. Song and X. Wang, *Coord. Chem. Rev.*, 2007, **251**, 111–141.

5   S. Shi, W. Ji, J. P. Lang and X. Q. Xin, *J. Phys. Chem.*, 1994, **98**, 3570–3572.

6   S. Shi, W. Ji, S. H. Tang, J. P. Lang and X. Q. Xin, *J. Am. Chem. Soc.*, 1994, **116**, 3615–3616.

7   J. Li, J. Zhang, M. G. Humphrey and C. Zhang, *Eur. J. Inorg. Chem.*, 2013, 328–346.

8   J. M. Garriga, R. Llusar, S. Uriel, C. Vicent, A. J. Usher, N. T. Lucas, M. G. Humphrey and M. Samoc, *Dalt. Trans.*, 2003, 4546–4551.

9   B. J. Coe, J. Fielden, S. P. Foxon, B. S. Brunschwig, I. Asselberghs, K. Clays, A. Samoc and M. Samoc, *J. Am. Chem. Soc.*, 2010, **132**, 3496–513.

10   C. C. Frazier, M. A. Harvey, M. P. Cockerham, H. M. Hand, E. A. Chauchard and C. H. Lee, *J. Phys. Chem.*, 1986, **90**, 5703–5706.

11   J. Dai, G.-Q. Bian, X. Wang, Q.-F. Xu, M.-Y. Zhou, M. Munakata, M. Maekawa, M.-H. Tong, Z.-R. Sun and H.-P. Zeng, *J. Am. Chem. Soc.*, 2000, **122**, 11007–11008.

12   G. Chatzikyriakos, I. Papagiannouli, S. Couris, G. C. Anyfantis and G. C. Papavassiliou, *Chem. Phys. Lett.*, 2011, **513**, 229–235.

13   D. Recatalá, A. L. Gushchin, R. Llusar, F. Galindo, K. A. Brylev, M. R. Ryzhikov and N. Kitamura, *Dalton Trans.*, 2013, **42**, 12947–55.

14   R. Llusar, S. Uriel, C. Vicent, J. M. Clemente-Juan, E. Coronado, C. J. Gomez-Garcia, B. Braida and E. Canadell, *J. Am. Chem. Soc.*, 2004, **126**, 12076–12083.

15   R. Llusar, S. Triguero, V. Polo, C. Vicent, C. J. Gómez-García, O. Jeannin and M. Fourmigué, *Inorg. Chem.*, 2008, **47**, 9400–9.

16   R. Llusar and C. Vicent, *Coord. Chem. Rev.*, 2010, **254**, 1534–1548.

17   D. Recatalá, R. Llusar, A. L. Gushchin, E. A. Kozlova, Y. A. Laricheva, P. A. Abramov, M. N. Sokolov, R. Gómez and T. Lana-villarreal, *ChemSusChem*, 2015, **8**, 148–157.

18   J. Chen, S. F. Lu, Z. X. Huang, R. M. Yu and Q. J. Wu, *Chem. - A Eur. J.*, 2001, **7**, 2002–2006.

19   M. D. Meienberger, K. Hegetschweiler, H. Rüegger and V. Gramlich, *Inorganica Chim. Acta*, 1993, **213**, 157–169.

20   H. Zimmermann, K. Hegetschweiler, T. Keller, V. Gramlich, H. W. Schmalle, W. Petter and W. Schneider, *Inorg. Chem.*, 1991, **30**, 4336–4341.

21   M. J. Mayor-López, J. Weber, K. Hegetschweiler, M. D. Meienberger, F. Joho, S. Leoni, R. Nesper, G. J. Reiss, W. Frank, B. A. Kolesov, V. P. Fedin and V. E. Fedorov, *Inorg. Chem.*, 1998, **37**, 2633–2644.

22   A. Gushchin, R. Llusar, D. Recatalá and P. Abramov, *Russ. J. Coord. Chem.*, 2012, **38**, 173–177.

23   A. V Virovets, A. L. Gushchin, P. A. Abramov, N. I. Alferova, M. N. Sokolov and V. P. Fedin, *J. Struct. Chem.*, 2006, **47**, 326–338.

24   M. N. Sokolov, P. A. Abramov, A. L. Gushchin, I. V Kalinina, D. Y. Naumov, A. V Virovets, E. V Peresypkina, C. Vicent, R. Llusar and V. P. Fedin, *Inorg. Chem.*, 2005, **44**, 8116–8124.

25   A. L. Gushchin, M. N. Sokolov, E. V. Peresypkina, A. V. Virovets, S. G. Kozlova, N. F. Zakharchuk and V. P. Fedin, *Eur. J. Inorg. Chem.*, 2008, 3964–3969.

26   G. Steimecke, H.-J. Sieler, R. Kirmse and E. Hoyer, *Phosphorous Sulfur Relat. Elem.*, 1979, **7**, 49–55.

27   T. K. Hansen, J. Becher, T. Jørgensen, K. S. Varma, Rajesh, M. P. C. Khedekar, J. Hynes and A. B. Smith, *Org. Synth.*, 1996, **73**, 270.

28   R. Llusar, S. Uriel, C. Vicent, J. M. Clemente-Juan, E. Coronado, C. J. Gómez-García, B. Braïda and E. Canadell, *J. Am. Chem. Soc.*, 2004, **126**, 12076–12083.

29   R. Llusar, S. Triguero, V. Polo, C. Vicent, C. J. Gómez-García, O. Jeannin and M. Fourmigué, *Inorg. Chem.*, 2008, **47**, 9400–9409.

30   A. L. Gushchin, Y. A. Laricheva, P. A. Abramov, A. V. Virovets, C. Vicent, M. N. Sokolov and R. Llusar, *Eur. J. Inorg. Chem.*, 2014, 4093–4100.

31   A. L. Gushchin, M. N. Sokolov, E. V Peresypkina, A. V Virovets, S. G. Kozlova, N. F. Zakharchuk and V. P. Fedin, *Eur. J. Inorg. Chem.*, 2008, 3964–3969.

32   M. Feliz, J. M. Garriga, R. Llusar, S. Uriel, M. G. Humphrey, N. T. Lucas, M. Samoc and B. Luther-Davies, *Inorg. Chem.*, 2001, **40**, 6132–6138.

33   R. L. Sutherland, *Handbook of Nonlinear Optics*, Marcel Dekker, Inc., 1996.

34   M. Feliz, R. Llusar, S. Uriel, C. Vicent, M. G. Humphrey, N. T. Lucas, M. Samoc and B. Luther-Davies, *Inorganica Chim. Acta*, 2003, **349**, 69–77.

35   M. Schwalbe, B. Schäfer, H. Görls, S. Rau, S. Tschierlei, M. Schmitt, J. Popp, G. Vaughan, W. Henry and J. G. Vos, *Eur. J. Inorg. Chem.*, 2008, 3310–3319.

36   A. Müller, E. Krickemeyer, A. Hadjikyriacou and D. Coucouvanis, in *Inorganic Syntheses*, ed. A. P. Ginsberg, John Wiley & Sons, Inc., 1990, vol. 27, pp. 47 – 51.

37   V. P. Fedin, M. N. Sokolov, Y. V. Mironov, B. A. Kolesov, S. V. Tkachev and V. Y. Fedorov, *Inorganica Chim. Acta*, 1990, **167**, 39–45.

38   *CrysAllis version 171.35.11.*

39   R. H. Blessing, *Acta Crystallogr. Sect. A Found. Crystallogr.*, 1995, **51**, 33–38.

40   L. Palatinus and G. Chapuis, *J. Appl. Crystallogr.*, 2007, **40**, 786–790.

41   G. M. Sheldrick, *Acta Crystallogr. Sect. A*, 2008, **64**, 112–122.

42   O. V Dolomanov, L. J. Bourhis, R. J. Gildea, J. A. K. Howard and H. Puschmann, *J. Appl. Crystallogr.*, 2009, **42**, 339–341.

43   L. J. Farrugia, *J. Appl. Crystallogr.*, 1997, **30**, 565.

44   P. Klingelhöfer, U. Müller, C. Friebel and J. Pebler, *Zeitschrift für Anorg. und Allg. Chemie*, 1986, **543**, 22–34.

45   R. Llusar, S. Triguero, S. Uriel, C. Vicent, E. Coronado and C. J. Gomez-Garcia, *Inorg. Chem.*, 2005, **44**, 1563–70.

27

Table 1. Selected average bond lengths (Å) for clusters $(Bu_4N)[(\mathbf{1} - \mathbf{4}) \cdot X]$, together with those of similar complexes (X = Cl or Br). Standard deviations are given in parentheses.

Cluster	Mo-Mo	Mo-(μ_3-S)	Mo-S_{ax}	Mo-S_{eq}	Mo-N	Mo-X	$S_{ax} \cdots X$
$(Et_4N)_3[Mo_3S_7Cl_6]$[44]	2.758(2)	2.346(3)	2.391(3)	2.483(3)	-	2.478(3)	2.94(7)
$(ET)_3[Mo_3S_7Br_6]$[45]	2.737(3)	2.344(6)	2.384(7)	2.466(7)	-	2.610(4)	3.05(2)
$(Bu_4N)[\mathbf{1} \cdot Cl]$	2.7502(6)	2.3531(12)	2.3852(13)	2.4861(14)	2.211(4)	2.4644(13)	2.93(4)
$(Bu_4N)[\mathbf{2} \cdot Br]$	2.7502(11)	2.359(3)	2.393(3)	2.481(3)	2.211(8)	2.6172(14)	3.05(5)
$(Bu_4N)[\mathbf{3} \cdot Br]$	2.7438(14)	2.3583(3)	2.391(3)	2.485(3)	2.225(10)	2.6212(17)	3.043(14)
$(Bu_4N)[\mathbf{4} \cdot Br]$	2.7414(7)	2.3553(15)	2.3958(16)	2.4852(17)	2.216(5)	2.6083(9)	3.04(8)

dtc = diethyldithiocarbamate; ET = bis(ethylendithio)tetrathiafulvalene

Table 2. Linear Optical and Optical-Limiting Data for $(Et_4N)_2[Mo_2O_2S_2(BPyDTS_2)_2]$[13] and complexes **1 – 7**.

cluster	Optical abs λ, nm (ε, 10^3 dm^3 mol^{-1} cm^{-1})						Cross section (10^{-18} cm^2)	
	λ_1 (ε_1)	λ_2 (ε_2)	λ_3 (ε_3)	Conc. (10^{-4} mol L^{-1})	λ_m (ε_m)^a	$F_{15\%}$ (J cm^{-2})^b	Ground state, σ_0	Excited state, σ_{eff}
Ref. [13]	341 (32)	423 (sh, 10.1)	525 (2.4)	27.2	570 (1590)	0.32	6.1	5.5
1	320 (sh, 11.1)	370 (sh, 5.3)	450 (2.3)	9.6	570 (310)	0.25	1.2	2.1
2	313 (sh, 21.1)	375 (sh, 7.5)	461 (3.7)	7.8	570 (830)	0.14	3.2	3.4
3	313 (sh, 16.5)	370 (sh, 5.2)	471 (sh, 2.4)	7.1	570 (790)	0.13	3.0	3.2
4	304 (sh, 14.9)	352 (sh, 6.1)	493 (sh, 1.9	7.2	570 (820)	0.20	3.2	3.9
5	307 (sh, 27.7)	-	497 (16.1)	3.2	570 (4410)	0.19	16.9	21.3
6	332 (sh, 17.1)	407 (sh, 7.4)	493 (10.2)	3.8	500 (9920)	0.31	37.9	37.0
					532 (6330)	0.30	24.2	23.4
					570 (3540)	0.22	13.5	15.3
					640 (1560)	0.19	5.9	9.3
7	311 (sh, 24.8)	335 (sh, 17)	500 (9.7)	5.5	570 (3060)	0.20	11.7	12.7

^{a} Measurement wavelength in nm (extinction coefficient at the measurement wavelength in dm^3 mol^{-1} cm^{-1}). ^{b} $F_{15\%}$ is defined as the incident fluence needed to reduce the transmittance through the sample by 15 %.

29

Table 3. Crystallographic data for (Bu$_4$N)[**1**·Cl]·3CH$_2$Cl$_2$, (Bu$_4$N)[**2**·Br]·(1/6)CH$_3$C$_6$H$_5$·(1/2)CH$_2$Cl$_2$, (Bu$_4$N)[**3**·Br]·CH$_3$C$_6$H$_5$·CH$_2$Cl$_2$ and (Bu$_4$N)[**4**·Br]

Compound	(Bu$_4$N)[**1**·Cl]·Solv	(Bu$_4$N)[**2**·Br]·Solv	(Bu$_4$N)[**3**·Br]·Solv	(Bu$_4$N)[**4**·Br]
Empirical formula	C$_{31}$H$_{53}$Cl$_{11}$Mo$_3$N$_3$S$_7$	C$_{29.7}$H$_{50}$Br$_5$ClMo$_3$N$_3$S$_7$	C$_{30}$H$_{30.5}$Br$_5$ClMo$_3$N$_3$S$_7$	C$_{26.75}$H$_{36.25}$Br$_5$Mo$_3$N$_3$S$_7$
Formula weight	1369.95	1395.96	1380.31	1311.63
Crystal system	Monoclinic	Triclinic	Monoclinic	Triclinic
a, Å	13.8174(2)	19.3605(3)	11.19024(19)	11.9690(3)
b, Å	19.3711(3)	25.9644(4)	32.5907(6)	12.7039(4)
c, Å	20.0877(3)	34.7600(5)	14.5892(3)	16.6526(5)
α°	90	71.8853(15)	90	71.325(3)
β°	103.4323(15)	76.3237(14)	108.499(2)	79.119(2)
γ°	90	76.3237(14)	90	65.163(3)
V, Å^3	5229.55(14)	15442.7(5)	5045.73(16)	2172.55(12)
T, K	200	200	200	200
Space group	P2$_1$/n	P-1	P2$_1$	P-1
Z	4	2	2	2
μ (Mo Kα), mm^{-1}	1.578	4.960	5.060	-
μ (Cu Kα), mm^{-1}	-	-	-	15.699
Reflections collected	50572	331374	48304	31156
Unique reflections	9195	60352	17681	8395
R_{int}	0.0332	0.0725	0.0338	0.0712
Goodness-of-fit on F^2	1.088	1.035	1.068	1.027
$R1^{[a]}$/$wR2^{[b]}$	0.0426 / 0.1056	0.0645 / 0.1673	0.0429 / 0.1225	0.0538 / 0.1534
$R1^{[a]}$/$wR2^{[b]}$ (all data)	0.0541 / 0.1188	0.1150 / 0.2007	0.0470 / 0.1256	0.0612 / 0.1654
Max/Min residual ρ /e·A^{-3}	1.54 / -0.90	3.08 / -1.08	3.29 / -0.58	1.75 / -1.46

$$[a]\ R1 = \sum ||F_0| - |F_1||/\sum F_0\ ;\ [b]\ wR2 = \left[\sum\left[w(F_0^2 - F_c^2)^2\right]/\sum\left[w(F_0^2)2\ \right]\right]^{1/2}$$